Samarium(III) and praseodymium(III) biosorption on Sargassum sp.: Batch study

Robson C. Oliveira, Claire Jouannin, Eric Guibal, Oswaldo Garcia

Samarium(III) and praseodymium(III) biosorption on *Sargassum* sp.: Batch study

Robson C. Oliveira [a,*], Claire Jouannin [b], Eric Guibal [b], Oswaldo Garcia Jr. [a]

[a] *Departamento de Bioquímica e Tecnologia Química, Instituto de Química, UNESP – Univ Estadual Paulista, Rua Prof. Francisco Degni, s/n, C. P. 14800-900, Araraquara, SP, Brazil*
[b] *Laboratoire Génie de l'Environnement Industriel, Ecole des Mines d'Alès (EMA), 6, avenue de Clavières, F-30319 Alès Cedex, France*

A B S T R A C T

This work evaluates the potential of a *Sargassum* biomass for the biosorption of Sm(III) and Pr(III) using synthetic solutions. Under selected experimental conditions (excess of sorbent), the biosorption kinetics were fast: 30–40 min were sufficient for the complete recovery of the metals. The kinetic profiles were modeled using the pseudo-second order rate equation. The second objective of this study was to evaluate the possibility to separate these metals. Biosorption isotherms and uptake kinetics for the two metals (in binary component solutions) were almost overlapped. The biomass did not show significant selectivity for any of these two metals, in batch reactor.

Keywords:
Sargassum sp.
Biosorption
Physicochemical modeling
Samarium
Praseodymium
Selectivity

1. Introduction

The recovery of heavy metals removal from dilute aqueous systems has required the development of new technologies for their concentration and separation [1,2]. Biosorption is a promising biotechnological alternative to conventional physicochemical processes such as: chemical precipitation, electrochemical separation, membrane separation, reverse osmosis, ion-exchange or adsorption resins [3–6]. Conventional methods involve either capital or high operational costs. They can also be associated to production of secondary residues that may cause environmental hazards or complexity in treatment or valorization [6,7]. The initial incentives for biosorption development in industrial process are the low cost of biosorbents, their high efficiency for metal removal (especially in low-concentration solutions), the biosorbent regeneration (and the potential metal recovery), the fast kinetics of adsorption and desorption, and the non-generation of secondary residues (or at least their limited environmental impact) [8].

Biosorption is a term that describes metal removal by passive binding in living and dead biomass from aqueous solutions in a mechanism that is not controlled by metabolic steps. The metal linkage is based on the chemical properties of the cellular envelope without requiring biologic activity [9–11]. The process occurs through interactions between metal species and actives sites (carboxyl, amino, sulfate, etc.) present on the cell wall [12]. Dead biomass is generally preferred since it limits the toxicity effects of heavy metals (which may accumulate at the surface of cell walls and/or in the cytoplasm) and the necessity to provide nutrients [2,13,14]. Alternatively, other biomaterials can be used for these purposes as biopolymers, activated sludge, agriculture wastes, etc. [15].

The mechanisms involved in metal accumulation on biosorption sites are numerous and their interpretation is made difficult the complexity of the biologic systems (presence of various reactive groups, interactions between the compounds, etc.). However, in most cases, metal binding proceeds through electrostatic interaction, surface complexation, ion-exchange, and precipitation, which can occur individually or combined [5,16].

Sargassum sp. biomass used in this work belongs to *Phaeophyta* group (brown seaweed). This alga is very abundant on the coasts of Brazil, Cuba, Australia, USA, and Asian Southeast [17]. Generally the cellular walls of *Phaeophyta* are constituted of a fibrillar skeleton and an amorphous matrix. The outer layer is an amorphous matrix that is linked to the fibrillar skeleton (mainly cellulose) via hydrogen bonding. The amorphous matrix is predominately formed by alginate, besides little amounts of fucoidan have been identified [18]. The alginate contributes to cellular wall resistance and flexibility [18,19]. Alginate carboxyl groups are the most abundant acidic groups (involved in metal binding): they represent approximately 70% of the titrated sites. The biosorption uptake is directly associated to the presence of carboxyl groups in the alginate polymer. The second functional group of the brown seaweed is constituted of sulfonic acid, present in the fucoidan: these groups may also contribute to biosorption [18]. Numerous studies have recently focused

* Corresponding author.
E-mail addresses: rcebinho@iq.unesp.br, rcebinho@yahoo.com.br (R.C. Oliveira), Eric.Guibal@mines-ales.fr (E. Guibal).

on the use of *Sargassum* biomass for the binding of several metals including Ni(II) [20], Cu(II) [21,22], and Zn(II) [23].

The group of rare earth metals (REs) comprises scandium, yttrium, and lanthanide series. The RE application fields are extensive, as a consequence of their peculiar spectroscopic and magnetic properties [23]. REs are of major interest for the development of several disciplines: coordination chemistry, organometallic compounds, luminescent compounds, catalysis, solid state chemistry, analytical and environmental chemistry, industrial applications, biology, and medicine. These metals are essential for manufacturing products such as lasers, superconductors, cracking catalysts for petroleum, miniaturized equipments, fluorescents lamps, satellites, phosphorus, ultraviolet radiation absorbers, permanent magnets, and electronic information storages [24,25].

Although REs are very abundant in the Nature, they present high market values due to expensive and complex processes for their separation and purification from mixtures because of their chemical similarities. These processes involve several steps of solvent extraction and/or ion-exchange resins, both with high costs [12,17]. The RE chemical similarities result from their electronic configurations: the trivalent state is the more stable thermodynamically in aqueous solution. Each lanthanide element has in its electronic configuration an inner shell with electrons in the $4f^n$ orbital shielded by an outer shell composed of electrons in orbitals $5s^2$, $5p^6$, $5d^{1-10}$, and $6s^2$. The differences among lanthanides elements are caused by electrostatic effect associated with the increase of shielded nuclear charge through electrons partial supply of 4f orbital (which results on lanthanide contraction of atomic and ionic radius along lanthanide series). This contraction is responsible for low differences on lanthanide chemical properties that allow metals separation by fractionating methods [23]. Only a few countries and multinational corporations have the complete technology for separation process of RE at industrial scale. For this reason despite their abundance, these metals have a considerable strategic value [25].

RE trivalent ions (Pearson hard acids: alkaline ions, alkaline earth ions, high oxidation state ions, species with low electronegativity and small size) tend to readily react with oxygen, sulfur, and phosphorus atoms (Pearson hard bases: electron donors, with high electronegativity and low polarizability), such as those found in the carboxyl groups of the cell wall of algae. Thereby it is important to establish the affinity differences among selected elements to propose a process for lanthanide separation and purification through biosorption [13,26].

This study is structured in three parts: (a) acid–base characterization of the biomass (potentiometric titration), (b) characterization of the biosorption kinetics (for single and binary solutions), and (c) determination of biosorption isotherms (for single and binary solutions). The final objective is to conclude on the efficiency of *Sargassum* sp. biomass to recover and separate samarium (Sm(III)) from praseodymium (Pr(III)) in dilute solutions. Previous investigation of REs biosorption on Sargassum biomass have shown that pH 5 is a good compromise for the sorption of these metals ions [10], based on metal speciation, and the deprotonation of the carboxylic groups present at the surface of the biosorbent. Though very slight variations can be observed around this target pH value for the different metal ions, selecting this pH facilitates the comparison of sorption behavior.

2. Materials and methods

2.1. Biomass pretreatment

Sargassum sp. biomass was collected on the coast of Rio Grande do Norte, Brazil. The biomass was grounded in a blender and the particles greater than 0.50 mm were selected. The biomass was washed three times for 1 h with demineralized water. The biomass was protonated with two washings in 0.020 mol L^{-1} HCl solutions for 1 h. The biosorbent was washed with demineralized water to remove the excess of H_3O^+, until reaching a pH close to 5.0. Finally, the biomass was dried overnight at 50 °C. The slightly acidic washing contributes to stabilize the biomass and prevent further leaching of organic compounds. In addition, this stabilization contributes to reduce pH variation that may occur during metal sorption. Strong pH variations may cause difficulties in the comparison of experimental results when different amounts of sorbent (which may interact with the solution through proton binding or proton release) are used. The conditions for acidic pre-treatment are soft enough to prevent a degradation of the biosorbent.

2.2. Rare earth solutions

RE stock solutions were prepared from Sm(III) and Pr(III,IV) oxides (both Aldrich Chemical Company 99.9%). The metal oxides were burned off at 900 °C for 3 h. They were subsequently dissolved in small amounts of concentrated HCl under heating before being diluted with demineralized water until final concentration of ~5.0 g L^{-1}. For these solutions, the RE concentrations were standardized by triplicate analysis using the complexometric titration with a standard solution of EDTA. The titration was carried out in buffer solution of acetate/acetic acid at pH 6.0 ± 0.2 using xylenol orange as the titration indicator (prepared in ethanol/water solution).

For metal biosorption experiments, the solutions used were prepared from dilutions of stock solutions and pH adjustment to 5.0 ± 0.1 with diluted HCl or NaOH solutions. The metal concentrations in both initial and withdrawn samples were determined by an Inductively Coupled Plasma Atomic Emission Spectrometer (ICP-AES JY 2000, Jobin-Yvon, Longjumeau, France). The ICP calibration was done utilizing RE standard solutions with three different concentrations and emission lines at 359.260 and 414.311 nm for Sm(III) and Pr(III), respectively.

2.3. Batch experiments

The biosorption experiments in batch systems were carried out in flasks containing 0.100 ± 0.020 g of biomass and 50 mL of RE solution for kinetics and isotherm, and 0.220 ± 0.040 g of biomass and 100 mL of RE solution for acid–base characterization. The flasks were maintained under agitation at 150 rpm and temperature of 20 °C (kinetics and isotherms) or 30 °C (acid–base characterization). All batch experiments were performed at least in triplicates. The calculation of the biosorption uptake (q) is given by the mass balance equation, Eq. (1).

$$q = \frac{(C_0 - C_F)}{M} V \quad (1)$$

where V (L) is the volume of metal solution in contact with the sorbent; C_0 and C_F (both in mmol L^{-1}) are the initial and final concentrations of the metal in the solution, respectively; and M (g) is the dry mass of the biosorbent.

2.4. Acid–base characterization of the biomass

The biomass was analyzed before and after metal biosorption. The pretreated biomass was protonated with HCl 0.10 mol L^{-1} (sorbent dosage, SD: 20.0 g L^{-1}), at 150 rpm and 20 °C for 1 h. The biomass was then filtered, washed with small volumes of demineralized water, and dried at 50 °C. The biosorption took place for 3 h. The initial metal concentrations of the RE solutions were 464 and 448 mg L^{-1} for Sm(III) and Pr(III), respectively. After being loaded with target metals the biomass was filtered, washed with small volumes of distilled water, and dried at 50 °C.

For each titration 0.200 ± 0.020 g of protonated or loaded biomass was dispersed in flasks with 100 mL of 1.0 mmol L^{-1} NaCl solution. Titration was carried out by addition of successive increments of standardized NaOH to the flask while the suspension was stirred under argon atmosphere. After each addition, the system was allowed to equilibrate until stable pH. The pH measurements were recorded using a Corning 430 pH meter. Potentiometric titrations were performed at least in triplicates.

Each endpoint of the potentiometric titration curves pH = f(NaOH) corresponds to a binding site in which protons are removed from the acidic functional groups to react with the hydroxyl ions added in solution. Thus, the acid dissociation constant of each functional group can be determined by the pK_a obtained from equivalent points through the determination of inflexion points. These points are determined plotting the first derivative curves of average pH titration data in function of the midpoint of successive amounts of NaOH added per mass of biomass (mmol g^{-1}). Each maximum peak of the curve dpH/dV = f(NaOH) corresponds to an inflexion point of the potentiometric titration curves. This procedure is used for evaluating the number of acidic groups present at the surface of the biomass [27].

The number of strong acid groups is determined from the first peak of the derivative curves while the total number of acid groups is determined from the final peak. The number of weak acid groups is then calculated by difference. The occupation of binding sites by metal ions after biosorption is calculated taking into account the total numbers of acid groups in the titration of biomass with and without metal binding.

2.5. Biosorption kinetics

For uptake kinetics (in mono-component solutions) the initial metal concentrations were 82 mg L^{-1} and 99 mg L^{-1} for Sm(III) and Pr(III), respectively. For uptake kinetics in binary component solutions, the initial metal concentrations

Table 1
Acid–base properties of protonated *Sargassum* sp. before and after Sm(III) and Pr(III) biosorption.

Material	Strong acid groups (mmol g^{-1})	Total amount of acid groups (mmol g^{-1})	Weak acid groups (mmol g^{-1})	Occupancy of binding sites (%)
Protonated biomass	0.15	1.77	1.62	–
Sm(III) – loaded biomass	0.07	1.26	1.19	29
Pr(III) – loaded biomass	0.07	1.18	1.11	33

were 48 mg L^{-1} and 49 mg L^{-1} (total metal concentration: 97 mg L^{-1}) for Sm(III) and Pr(III), respectively. Samples were collected at distinct contact times (between 0 and 480 min) and filtered for the analysis of residual metal concentrations.

The biosorption kinetics of *Sargassum* sp. was evaluated by the pseudo-second-order rate equation reported on Eq. (2). The different parameters of the model were calculated by the linear regression using Eq. (3).

$$\frac{dq}{dt} = k_2(q_{EQ} - q_t)^2 \tag{2}$$

$$\frac{t}{q_t} = \frac{1}{k_2 q_{EQ}^2} + \frac{1}{q_{EQ}}t = \frac{1}{v_0} + \frac{1}{q_{EQ}}t \tag{3}$$

where q_t and q_{EQ} (both in mmol g^{-1}) are the biosorption uptake at time t (min) and at equilibrium, respectively; k_2 (g $mmol^{-1}$ min^{-1}) is the constant of the pseudo-second order rate equation; and v_0 (mmol g^{-1} min^{-1}) is the initial adsorption velocity.

The profile of the total metal biosorption uptake was performed by the sum of the samarium and praseodymium individual biosorption uptake, i.e. $q_{Sm} + q_{Pr}$. The constant of pseudo-second order rate equation was obtained from this profile using again Eq. (3). This corresponds to the cumulative constant of pseudo second-order rate equation ($k_{2,CUM}$). The experimental value of $k_{2,CUM}$ was compared with those obtained from the semi-empirical equation (4) (for comparison with experimental results).

$$k_{2,CUM} = \frac{1}{(1/k_{2,Sm}) + (1/k_{2,Pr})} \tag{4}$$

where $k_{2,Sm}$ and $k_{2,Sm}$ are the individual constants of pseudo-second order rate equation for Sm(III) and Pr(III), respectively.

2.6. Biosorption isotherms

Biosorption isotherms were established by mixing for hours a given amount of biomass with a volume of solution containing different initial metal concentrations. For Sm(III) and Pr(III) single-component solutions the initial metal concentrations varied between 0 and 1500 mg L^{-1}; while for Sm(III) and Pr(III) sorption in binary component solutions, they varied between 0 and 750 mg L^{-1} for each metal (total metal concentration between 0 and 1500 mg L^{-1}). The biosorption of single solutions was analyzed with the model of Langmuir (using Eq. (5)). The parameters describing this model were calculated by linear regression following Eq. (6).

$$q = \frac{q_{MAX} b C_{EQ}}{1 + b C_{EQ}} \tag{5}$$

$$\frac{C_{EQ}}{q} = \frac{1}{b q_{MAX}} + \frac{1}{q_{MAX}} C_{EQ} \tag{6}$$

where q and q_{MAX} (both mmol g^{-1}) are the biosorption uptake and the maximum biosorption uptake at saturation of the monolayer, respectively; b (L g^{-1}) is a constant that represents the affinity between the metal and the biomass in the Langmuir model; and C_{EQ} (g L^{-1}) is the equilibrium metal concentration.

The biosorption isotherms of the binary solutions were analyzed with the Langmuir multi-component competitive model shown in Eqs. (7) and (8), for Sm(III) and Pr(III), respectively.

$$q_{Sm} = \frac{q_{MAX,Sm} b_{Sm} C_{EQ,Sm}}{1 + b_{Sm} C_{EQ,Sm} + b_{Pr} C_{EQ,Pr}} \tag{7}$$

$$q_{Pr} = \frac{q_{MAX,Pr} b_{Pr} C_{EQ,Pr}}{1 + b_{Sm} C_{EQ,Sm} + b_{Pr} C_{EQ,Pr}}, \tag{8}$$

Theoretically, the q_{MAX} and b parameter applied in Eqs. (7) and (8) are described by the values found in the single-component solutions (Eqs. (5) and (6)). However the biosorption on binary component solutions can implicate a change in the affinity for each component, which can be obtained by the mathematical arrangement of Eqs. (7) and (8); and their linear regressions, according to Eqs. (9) and (10) [28].

$$C_{EQ,Sm}\left(\frac{q_{MAX,Sm}}{q_{Sm}} - 1\right) = \frac{1}{b_{Sm}} + \frac{b_{Pr}}{b_{Sm}} C_{EQ,Pr} \tag{9}$$

$$C_{EQ,Pr}\left(\frac{q_{MAX,Pr}}{q_{Pr}} - 1\right) = \frac{1}{b_{Pr}} + \frac{b_{Sm}}{b_{Pr}} C_{EQ,Sm} \tag{10}$$

$q_{MAX,i}$ values correspond to the values obtained from single solutions. Eqs. (9) and (10) were called approximations for Sm(III) and Pr(III), respectively.

The profile of total metal biosorption uptake (sum of Sm(III) and Pr(III) individual sorption capacities) was also plotted as a function of total metal concentration. Eqs. (5) and (6) were used to determine the q_{MAX} and b parameters for individual and total biosorption uptakes by simple mathematical adjustment, ignoring the physicochemical effects of competition. This approach was called Langmuir uncompetitive model. These results were used to compare the cumulative affinity constant of Langmuir (b_{CUM}) and the affinity coefficient calculated by the semi-empirical equation (11).

$$b_{CUM} = \frac{1}{(1/b'_{Sm}) + (1/b'_{Pr})} \tag{11}$$

where b'_{Sm} and b'_{Pr} are the affinity constants of Langmuir for Sm(III) and Pr(III), respectively, obtained by the direct application of Eq. (6) for binary component solutions.

The theoretical model, the mathematically modified Langmuir multi-component competitive models, and the Langmuir uncompetitive model were compared by the root mean square error (RMSE) described by Eq. (12).

$$\mathrm{RMSE} = \sqrt{\frac{\sum_{i=1}^{n}[q_{i,MODEL} - q_{i,EXP}]^2}{n}} \times 100\%, \tag{12}$$

where $q_{i,MODEL}$ and $q_{i,EXP}$ are the modeling and experimental data of the biosorption uptake; for i data; n being the total number of experimental data.

3. Results and discussion

3.1. Acid–base characterization of the biomass

The potentiometric titrations of the biomass (after protonation) with and without metal loading are reported in Fig. 1. A significant dispersion of data is observed when repeated; however, this dispersion is less marked than the dispersion observed with non-protonated (i.e., raw) biomass (not shown). The acid treatment contributes to remove some leachable materials (organic compounds, carbonate-based materials) that could influence acid–base properties. These materials being unequally distributed in the material this may explain the greater spread of data for raw material (compared to treated biomass).

The first derivative plots of average titration curves are shown in Fig. 2. The dispersion of data introduced a number of secondary peaks that make difficult the identification of the inflexion points for strong acid groups and total acid groups. Table 1 summarizes the characteristics of the protonated *Sargassum* sp. biomass before and after metal biosorption.

The strong acid groups counted for only 0.15 mmol g^{-1} on protonated biomass, and decreased to 0.07 mmol g^{-1} after the biosorption of either Sm(III) or Pr(III). These groups of lowest pK_a have been identified as the sulfonate groups of the fucoidan (actually ester sulfate groups), which are present on the cell wall of brown seaweeds [28]. Weak acid groups are mainly constituted by carboxylate groups from alginate compounds, which represent more than 90% of total acid groups (i.e., 1.62 mmol g^{-1}). This value remains in the same order of magnitude compared with other brown algae cited in the literature: 1.95 mmol g^{-1} for *Sargassum fluitans* and 2.20 mmol g^{-1} for *Cystoseira baccata* [29,30]. After metal biosorption the titration identified 1.19 and 1.11 mmol g^{-1} of weak acid groups for Sm(III) and Pr(III), respectively. Thereby only around 30% of the acid groups were involved in metal binding. The differences observed after metal biosorption were not very marked between Sm(III) and Pr(III); therefore the biomass appears to have comparable efficiency for the biosorption of these two REs.

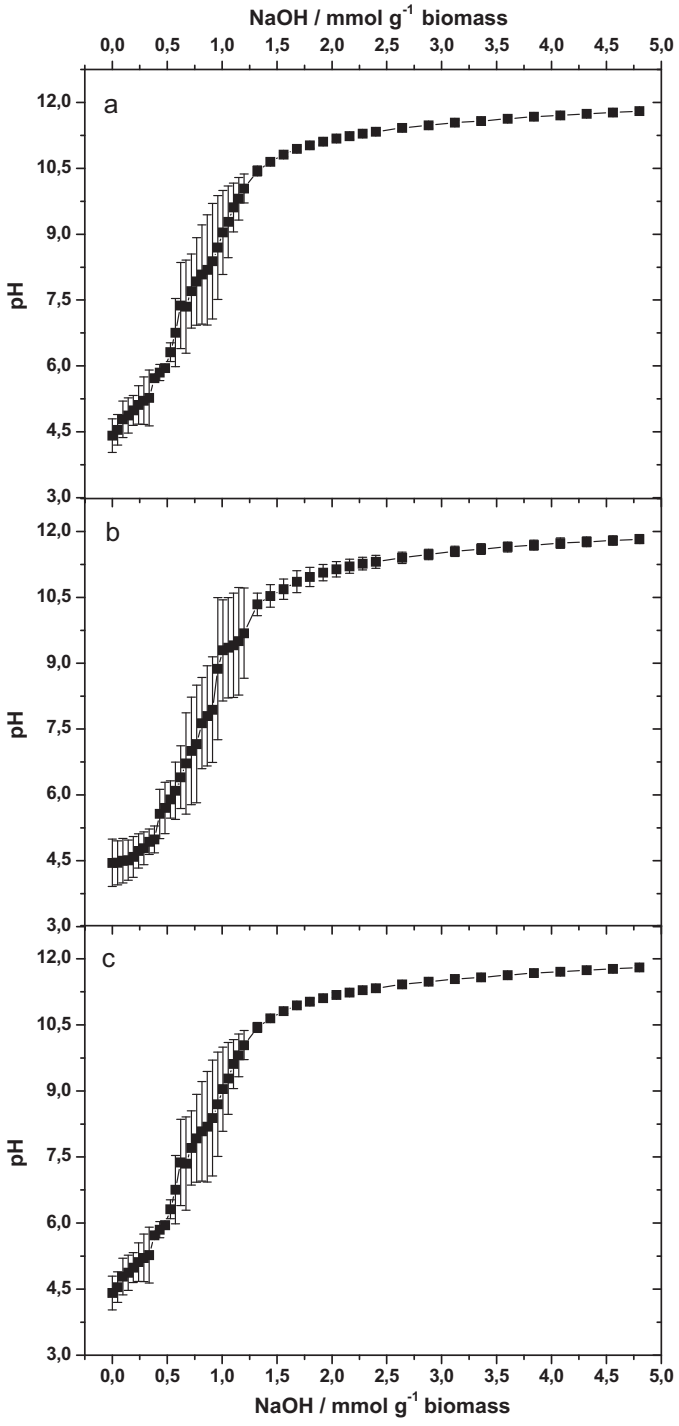

Fig. 1. Potentiometric titration curves of protonated *Sargassum* sp.: (a) without metal, (b) after biosorption of Sm(III), and (c) after biosorption of Pr(III).

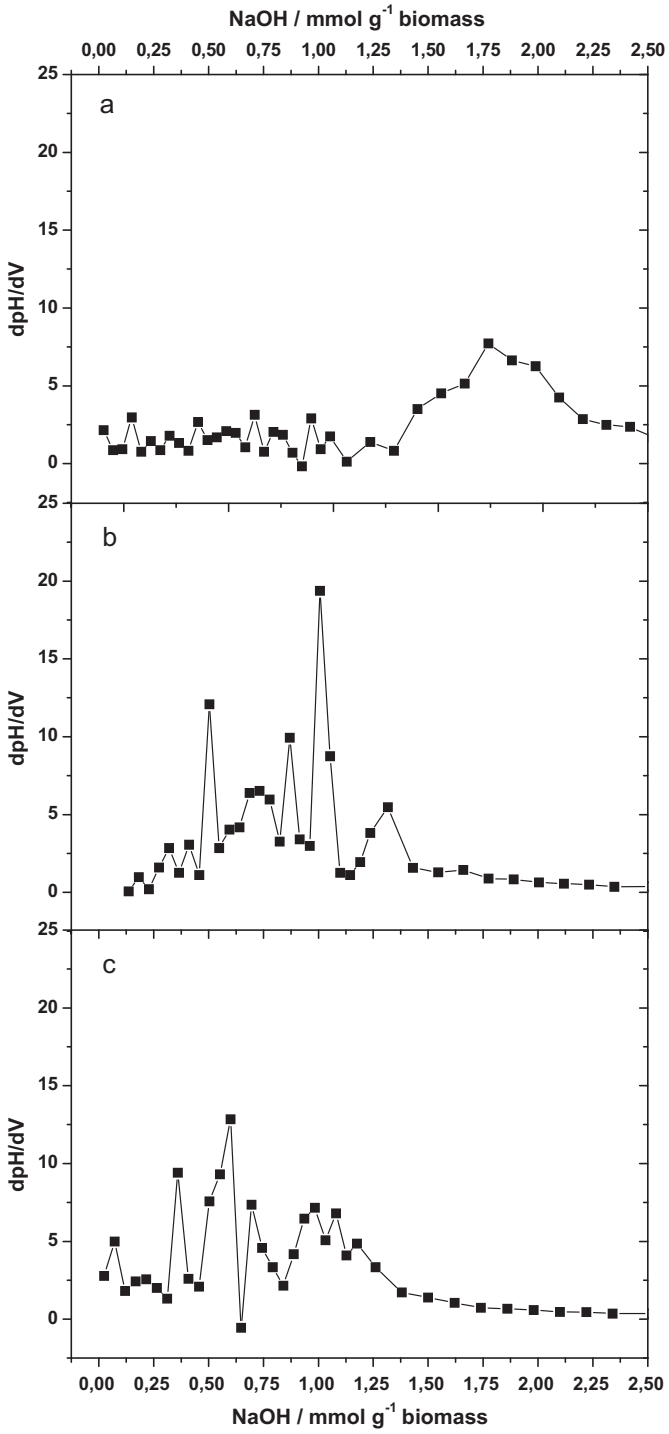

Fig. 2. First derivative curves of average pH titrations of protonated *Sargassum* sp.: (a) without metal, (b) after biosorption of Sm(III), and (c) after biosorption of Pr(III).

3.2. Biosorption kinetics

Fig. 3 shows the biosorption kinetics in single solutions for Sm(III) and Pr(III) modeled by the pseudo-second order rate equation. The kinetics parameters obtained are reported in Table 2. These parameters were compared to others obtained under the same experimental conditions by Oliveira and Garcia Jr. [31] for the biosorption of La(III), Nd(III), Eu(III), and Gd(III) (Table 2).

Table 2 shows that the modeling fitted well experimental data ($R^2 > 0.98$). Fig. 3 is characterized by a sharp increase the metal uptake q for the first 30–40 min of contact. The comparison of results obtained for the six RE metals (Table 2) does not show a clear trend for the evolution of the kinetic characteristics for the different metal ions. More specifically, it was not possible correlating this evolution with the chemical characteristics (such as metal molecular weight or effective ionic radii in RE cations III) of these different metals (Table 3) [32]. Though some differences were observed for k_2 and v_0 values obtained, these differences are not statistically differentiable because of the high similarity among the kinetic profiles and a little number of data collected. For instance, the k_2 and v_0 results for Pr(III) were greater than other metals; however, the

Table 2
Physicochemical parameters and correlation coefficients from biosorption kinetics for Sm(III), Pr(III), La(III), Nd(III), Eu(III), and Gd(III) single solutions by *Sargassum* sp. described by the pseudo-second-order kinetic model.

Metal	q_{EQ} (mmol g^{-1})	k_2 (g mmol^{-1} min^{-1})	v_0 (mmol g^{-1} min^{-1})	R^2	Reference
Sm(III)	0.34 ± 0.01	0.40 ± 0.04	0.048 ± 0.006	0.988	This work
Pr(III)	0.29 ± 0.01	0.78 ± 0.07	0.065 ± 0.007	0.998	This work
La(III)	0.37	0.31	0.042	0.996	[28]
Nd(III)	0.37	0.31	0.043	0.997	[28]
Eu(III)	0.31	0.56	0.056	1.000	[28]
Gd(III)	0.35	0.42	0.050	0.999	[28]

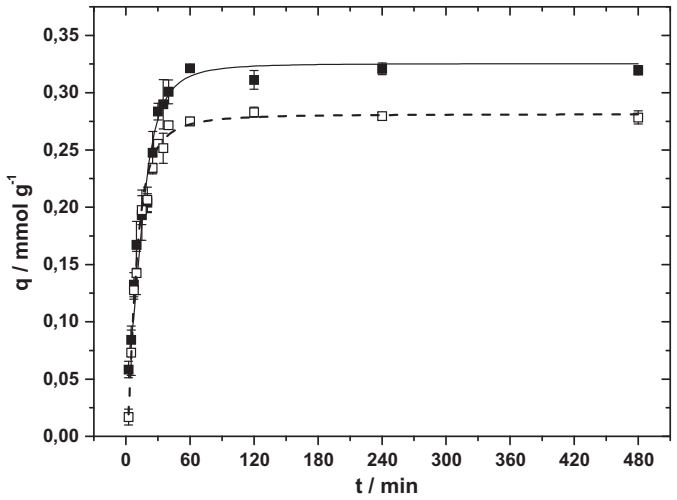

Fig. 3. Biosorption kinetics for Sm(III) and Pr(III) single solutions by *Sargassum* sp. described by the pseudo-second-order kinetics model. Symbols: (–■–) Sm(III) and (–□–) Pr(III).

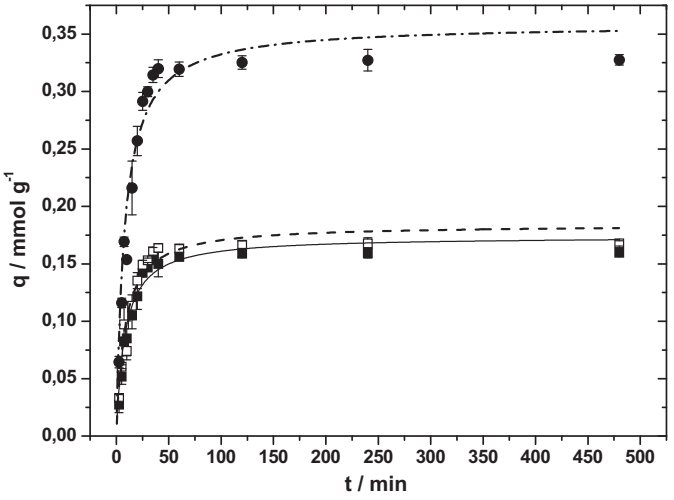

Fig. 4. Biosorption kinetics for Sm(III) and Pr(III) binary solution by *Sargassum* sp. described by the pseudo-second-order kinetics model. Symbols: (–■–) Sm(III), (–□–) Pr(III), and (–·–●–·–) Sm(III) + Pr(III).

Table 3
Molecular weight and effective ionic radii in the rare earth compared [32].

Element	Atomic number	Molecular weight	Effective ionic radii III (Å)		
			CN[a] = 6	CN[a] = 8	CN[a] = 12
La	57	138.91	1.045	1.180	1.320
Pr	59	140.91	0.997	1.140	1.290
Nd	60	144.24	0.983	1.120	1.276
Sm	62	150.36	0.958	1.090	1.260
Eu	63	151.96	0.947	1.070	1.252
Gd	64	157.25	0.938	1.060	1.246

[a] CN is the coordination number of the rare earth cations (III).

embedded experimental errors are too high for allowing a more accurate analysis.

Fig. 4 shows the biosorption kinetics in binary component solutions for Sm(III) and Pr(III) (experimental points) and their modeling (curves) using the pseudo-second order rate equation. The kinetic parameters obtained are reported in Table 4: the pseudo-second order rate equation also presented relevant correlation coefficients ($R^2 > 0.98$) for the binary component solutions. The model fitted well experimental data (Fig. 4) but some discrepancies appeared for contact times greater than 60 min. Both metals presented similar behavior in binary solutions, as shown in Table 4 and Fig. 4, where the curves for Pr(III) and Sm(III) are almost overlapped. The biosorbent does not mark a clear preference for any of the two metals during uptake kinetics.

The parameter $k_{2,CUM}$ for the total metal biosorption uptake (cumulative uptake kinetics: Sm(III) + Pr(III)), was calculated using Eq. (4). The value found was 0.35 ± 0.01 g mmol^{-1} min^{-1}, which is consistent with the experimental value (i.e., 0.36 g mmol^{-1} min^{-1}, Table 4). This means that under selected experimental conditions, the semi-empirical relation can be used to predict the $k_{2,CUM}$ from the k_2 individual values.

3.3. Biosorption isotherms

Fig. 5 shows the biosorption isotherms in single solutions for Sm(III) and Pr(III). Experimental data are modeled using the Langmuir equation. Table 5 records the parameters of the model for Sm(III) and Pr(III). Table 5 also reports the parameters of the Langmuir equation for the sorption isotherms obtained with the same biomass for the recovery of La(III), Nd(III), Eu(III), and Gd(III) [31].

Langmuir equation fitted well sorption isotherms for both Sm(III) and Pr(III), as shown by the correlation coefficients ($R^2 > 0.99$). Additionally, it is noteworthy that the shape of the biosorption isotherms (Fig. 5) approaches the profile of irreversible isotherms: the initial slope is very steep and the equilibrium plateau is reached at low residual concentration. This can be

Table 4
Physicochemical parameters and correlation coefficients from biosorption kinetics for Sm(III) and Pr(III) binary solution by *Sargassum* sp. biomass described by the pseudo-second-order kinetic model.

Metal	q_{EQ} (mmol g^{-1})	k_2 (g mmol^{-1} min^{-1})	v_0 (mmol g^{-1} min^{-1})	R^2
Sm(III)	0.18 ± 0.01	0.72 ± 0.01	0.022 ± 0.001	0.992
Pr(III)	0.18 ± 0.01	0.69 ± 0.02	0.023 ± 0.001	0.987
Sm(III) + Pr(III)	0.36 ± 0.01	0.36 ± 0.01	0.046 ± 0.002	0.988

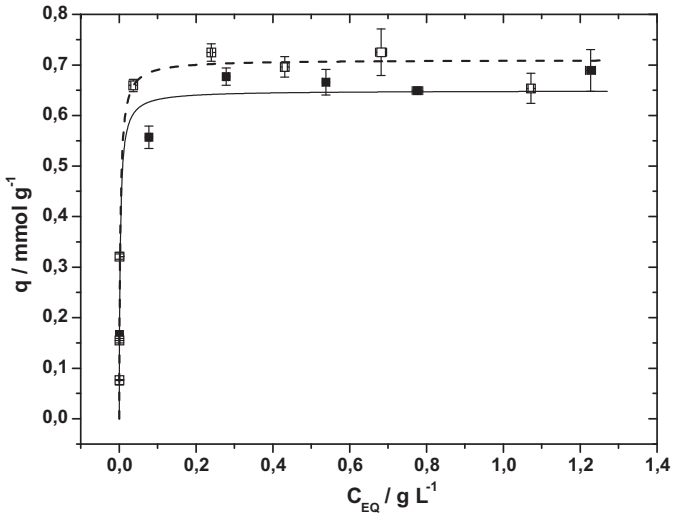

Fig. 5. Biosorption isotherms for Sm(III) and Pr(III) single solutions by *Sargassum* sp. described by the Langmuir adsorption model. Symbols: (–■–) Sm(III) and (–□–) Pr(III).

Table 5
Physicochemical parameters and correlation coefficients from biosorption isotherms for Sm(III), Pr(III), La(III), Nd(III), Eu(III), and Gd(III) single solutions by *Sargassum* sp. described by the Langmuir adsorption model.

Metal	q_{MAX} (mmol g^{-1})	b (L g^{-1})	R^2	Reference
Sm(III)	0.65 ± 0.01	354.9 ± 39.8	0.992	This work
Pr(III)	0.71 ± 0.02	345.1 ± 42.3	0.990	This work
La(III)	0.66	837.3	1.000	[31]
Nd(III)	0.70	192.5	0.999	[31]
Eu(III)	0.63	678.3	1.000	[31]
Gd(III)	0.67	183.1	1.000	[31]

correlated to the great affinity of Sm(III) and Pr(III) for the biosorbent. The values of maximum biosorption uptake (saturation of the monolayer) were of 0.65 for Sm(III) and 0.71 for Pr(III) (Table 5). Comparing these sorption capacities to the carboxylic acid content (i.e., 1.62 mmol g^{-1}, Table 1), the molar ratio carboxylic group/metal varied between 2.3 and 2.5, below the theoretical 3:1 molar ratio expected for respecting the stoichiometry of ion exchange between the trivalent cations and the protons on carboxylic acid groups. This probably means that other functional groups may be involved in the binding of RE: RE trivalent cations bind to carboxylic groups of alginate-based compounds through an ion exchange mechanism while other components of the cell wall could contribute to complementary sorption (including fucoidan compounds). The diversity of functional groups present in microorganisms (compared to pure biopolymers such as alginate) may explain some discrepancies in the stoichiometric ratios. Rare earths have affinity for a number of reactive groups (the strength being controlled by Pearson's rules, hard & soft acid & base theory). For example, in the case of the yeast *Candida utilis*, it was possible correlating the affinity of the biosorbent for a series of REs to the phosphorus content of the cell wall [33]. The chemical modification of the surface, the extraction of target compounds directly influenced metal biosorption.

Table 6
Rare earth biosorption by *Sargassum* sp. biomass and biosorption parameters for the Langmuir adsorption model reported in some studies.

Metal	Biomass	q_{MAX} (mmol g^{-1})	Reference
Eu	*Sargassum polycystum*	0.8–0.9	[27]
La	*Sargassum fluitans*	0.53–0.73	[17]
	Sargassum polycystum	0.8–0.9	[26]
	Sargassum sp.	0.54[a]	[35]
	Sargassum sp.	0.44[a]	[36]
Nd	*Sargassum* sp.	0.53[a]	[17]
	Sargassum sp.	0.41[a]	[36]
Yb	*Sargassum polycystum*	0.7–0.9	[26]

[a] Calculated from original results that were in other dimensional units.

The Langmuir parameters (for single-component solutions) for Sm(III) and Pr(III) can be compared to the values obtained with other REs (Table 5) [31]. The maximum biosorption uptake (q_{MAX}) systematically varied between 0.63 and 0.71 mmol g^{-1}; the present study is thus consistent with the sorption capacities of *Sargassum* sp. for other REs. These values are also consistent with other studies regarding RE biosorption by different *Sargassum* species (Table 6). In the case of Pr(III) biosorption on *Pseudomonas aeruginosa*, the sorption capacity reached up to 0.94 mmol Pr g^{-1} [34]: this is slightly higher than the sorption capacities found in this study. Actually, in this case the sorption proceeds through a dual mechanism involving ion exchange reaction on the functional groups present at the surface of the biosorbent and the biologically mediated transfer of the RE into the cytoplasmic compartment. The Langmuir affinity coefficient (i.e., b) varies between 183.1 L g^{-1} and 837.3 L g^{-1}; this means that the affinity of this biosorbent significantly depends on the RE. The affinity coefficient follows the sequence: Gd < Nd < Pr < Sm < Eu < La. Previous section on uptake kinetics showed that it was not possible correlating the kinetic parameter with the characteristics of the RE. A similar conclusion can be reached considering the affinity coefficient: the ranking of affinity coefficient cannot be connected to the properties of the REs such as the ionic radius, etc. (Table 3) [32].

Despite the differences in the values of the affinity coefficient, the isotherm profiles appear quite comparable and probably not statistically differentiable. For this reason it seems that the separation of the REs will be difficult. In order to verify this hypothesis sorption isotherms were performed in binary component solutions (Fig. 6). This figure shows experimental data together with curve modeling using the theoretical, mathematically modified, and uncompetitive Langmuir equations for Sm(III), Pr(III) (alone and in binary component solutions). The results for theoretical Langmuir model (Eqs. (7) and (8)) are shown in Table 5 for single component solutions. The Langmuir affinity parameters (b) obtained in

Table 7
Parameters and correlation coefficients related to mathematically modified and uncompetitive Langmuir models in the Sm(III) + Pr(III) binary solution.

Langmuir model	Condition	b_{Sm} (L g^{-1})	b_{Pr} (L g^{-1})	R^2	b_{Sm+Pr} (L g^{-1})	R^2
Mathematically modified	Sm(III) approximation	478.5 ± 41.0	372.9 ± 13.3	0.991	–	–
	Pr(III) approximation	380.1 ± 18.4	325.7 ± 44.2	0.974	–	–
Uncompetitive	Linear regression	684.0 ± 67.7	1379 ± 187.0	0.945[a]/0.950[b]	410.4 ± 0.4	0.991
	Cumulative data	–	–	–	447.6 ± 50.8[c]	–

[a] For Sm(III).
[b] For Pr(III)
[c] Extrapolated value from modeled curve.

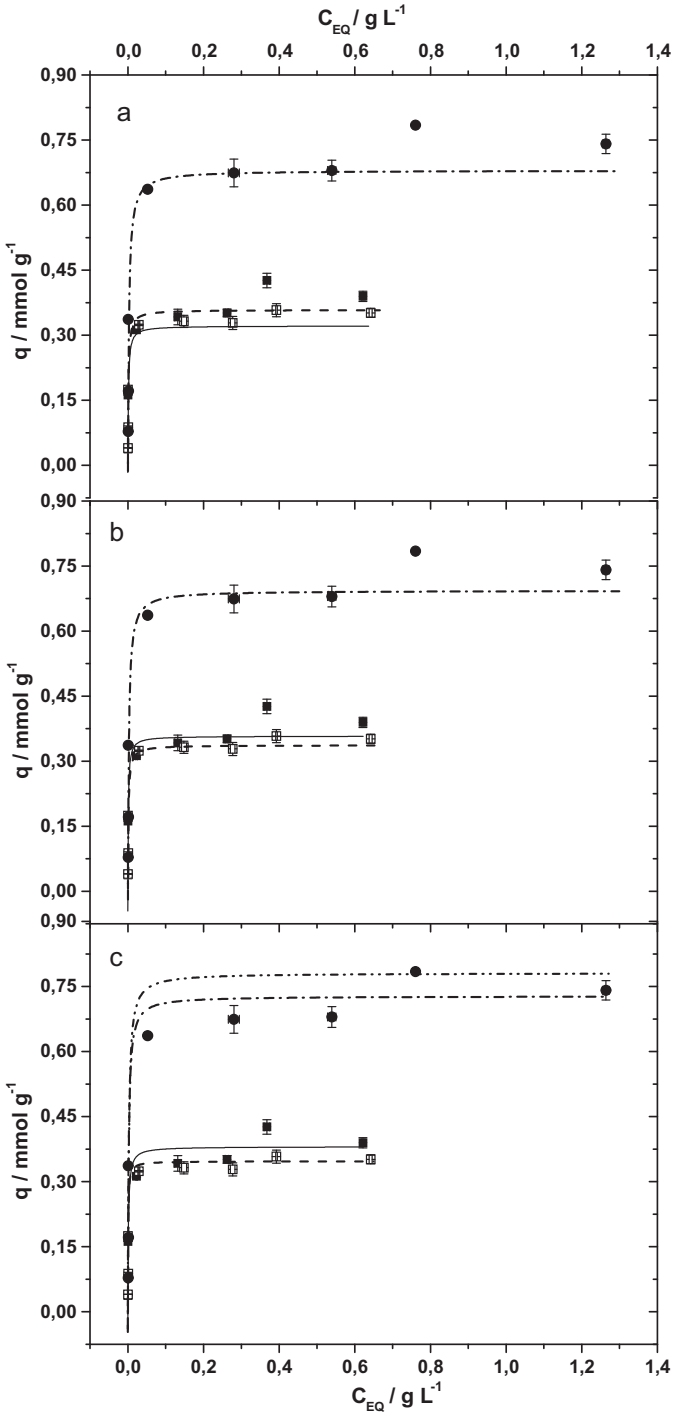

Fig. 6. Biosorption isotherms for Sm(III) and Pr(III) binary solution by *Sargassum* sp. described by the Langmuir model: (a) curves plotted for the theoretical model; (b) curves plotted for the mathematically modified model; and (c) curves plotted for the uncompetitive model. Symbols: (–■–) Sm(III), (–□–) Pr(III), (-·-●-·-) Sm(III) + Pr(III) from cumulative data of biosorption uptake, and (-···●···-) Sm(III) + Pr(III) from parameters obtained of linear regression.

the mathematically modified Langmuir model for Sm(III) and Pr(III) approximations (Eqs. (9) and (10)) and for uncompetitive Langmuir model (Eqs. (5) and (6)) are summarized in Table 7. The comparison among the curves for these models was performed by the root mean square error (RMSE) in Table 8.

Fig. 6 shows that the individual and total metal biosorption isotherm profiles, for binary component solutions, display a relatively close behavior in the curve shape compared with the single

Table 8
Root mean square error of the theoretical, mathematically modified, and uncompetitive Langmuir models for the biosorption uptake in the Sm(III) + Pr(III) binary solution.

Langmuir model	RMSE (%)		
	Sm(III)	Pr(III)	Sm(III) + Pr(III)
Theoretical	6.02	4.60	8.25
Mathematically modified	4.22	4.18	7.89
Uncompetitive	4.24	5.07	9.70[a]/8.36[b]

[a] From curve modeled with the parameters obtained of linear regression.
[b] From curve modeled with the cumulative data of biosorption uptake.

solutions. Furthermore, the total metal uptake shows similar value (about 0.70 mmol g^{-1}) that indicates the complete saturation of the active sites. The experiments on single solutions showed that the biomass has greater affinity (b) for Sm(III) and greater maximum biosorption uptake (q_{MAX}) for Pr(III) (Table 5). For the theoretical model, Fig. 6(a) shows that contrary to the results expected from single-component solutions the maximum biosorption uptake was greater for Sm(III) than for Pr(III).

The mathematically modified Langmuir model (Fig. 6(b)) shows good correlation ($R^2 > 0.97$) with experimental data for both Sm(III) and Pr(III) (Table 7). These values indicate that the modified model can be applied for the biosorption of REs and they suggest a better affinity of Sm(III) than Pr(III) for binding sites. Indeed, the b parameter values reported in Table 7 for Sm(III) are greater than for Pr(III), consistently with data obtained with single-component solutions (Table 5). Though slightly different, the values of the affinity coefficient (i.e., b) in binary solutions are of the same order of magnitude than the values obtained with single-component solutions. This is contrary to the expected trends corresponding to the theoretical model (where the q_{MAX} for Pr(III) should be greater than for Sm(III), Table 5). This difference can be explained by: (a) the greater biomass affinity for Sm(III), which, in turn, limits Pr(III) maximum biosorption, and/or (b) the displacement of Pr(III) by Sm(III).

Fig. 6(c) shows the uncompetitive Langmuir model. This model does not fit well experimental data in the monometallic biosorption profiles ($R^2 < 0.95$) (Table 7). Moreover, the parameter b for these profiles was very high at saturation for each metal. The affinity coefficient is smaller (about 0.35–0.40 mmol L^{-1}) than those in single component solutions (0.65 mmol L^{-1} for Sm(III) and 0.71 mmol L^{-1} for Pr(III)). The parameter b for the total metal biosorption was suitable ($R^2 > 0.99$) when estimated by the linear regression from the entire experimental range (Table 7). Comparatively the same parameter estimated from the cumulative data of the individual Sm(III) and Pr(III) biosorption uptakes showed similar value (Table 7). Both results are in agreement with the cumulative affinity constant of Langmuir (b_{CUM}) calculated by the semi-empirical equation (11) (where b'_{Sm} and b'_{Pr} are related to the individual Sm(III) and Pr(III) biosorption uptakes, respectively, Table 7), which corresponds to 457.2 L g^{-1}. As for biosorption kinetics, the semi-empirical relation can be used to predict the b_{CUM} from the b individual values (under selected experimental conditions).

Based on Fig. 6, the best model for simulating experimental data was the mathematically modified Langmuir model. Indeed the analysis of the models through the RMSE reveals that the mathematically modified model presents lower deviations than the other models. This means that in binary component solutions a slight competition occurs between the metals, with affinities which are different from those observed in single-component solutions.

Considering the results obtained in kinetics and sorption isotherms from both single-component and binary solutions it appears that Sm(III) and Pr(III) are equivalently adsorbed without

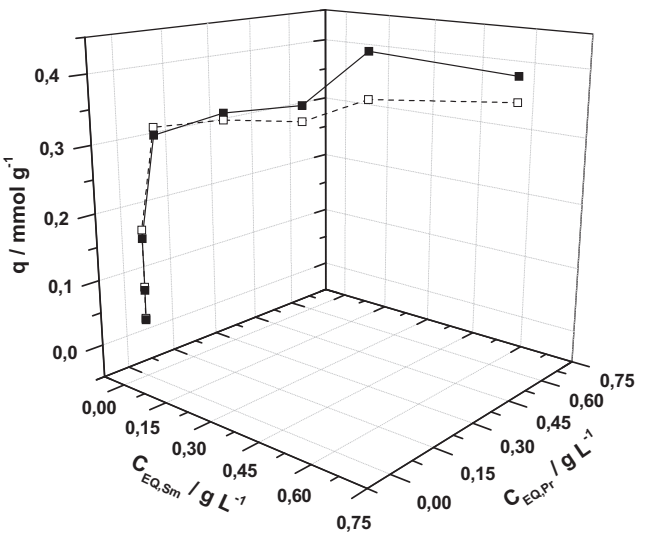

Fig. 7. 3-D schematic projections of the biosorption isotherms for Sm(III) and Pr(III) binary solution by *Sargassum* sp. Symbols: (–■–) samarium and (–□–) praseodymium. Note: the graphic was plotted with the average values of equilibrium concentration and biosorption uptake.

significant difference; this makes difficult the separation of these REs. This can be more easily visualized in the 3-D projection of binary biosorption isotherms shown in Fig. 7. The isotherms for Sm(III) and Pr(III) are very close and the slight differences observed at high metal concentrations do not appear to be relevant and significant for an effective separation of these metals. Additionally, the weak efficiency in metal separation is confirmed by the equilibrium molar ratio (on the biomass), given by q_{Sm}/q_{Pr}: the value was systematically close to 1 (i.e., 1.02 ± 0.10).

The two metals can be seen as equivalently adsorbable on the biomass and probably the biosorbent will not bring enough selectivity for an efficient separation of Sm(III) from Pr(III), at least on the basis of equilibrium distribution of metals ions, at least in the batch mode.

4. Conclusions

Sargassum biomass can be efficiently used for the binding of Sm(III) and Pr(III). The main reactive functions are probably the carboxylic groups present in alginate, the main component of macroalgae cell wall. The carboxylic groups (pK_a close to 3–3.5) being deprotonated at pH 5, the adsorption probably proceeds through electrostatic attraction followed by ion-exchange (with the protons from carboxylic groups). The biosorption uptake approaches 0.70 mmol g^{-1}; the molar ratio R-COOH/RE is close to 2.3. The pseudo-second-order equation fitted well uptake kinetics that were very similar for Sm(III) and for Pr(III) in both single and binary solutions. The biosorption isotherms can be described by the Langmuir equation: the steep initial slope indicates a strong affinity of the biomass for the metals. The biosorption isotherms in mono-component and binary solutions were very close for Sm(III) and Pr(III). The biomass cannot be used for a pre-concentrative separation of these metal ions. Experiments in fixed-bed dynamic systems (to be discussed in future work) would be necessary to confirm this conclusion, since they can enhance the separation effect.

Acknowledgements

The authors thank to European Commission for the financial support for the Project BIOPROAM (Bioprocesos: Tecnologías limpias para la protección y sustentabilidad del medio ambiente) of the ALFA Research Program (Contract Number: AML/190901/06/18414/II-0548-FC-FA). R. C. Oliveira and O. Garcia Jr. also thank to Coordenação de Aperfeiçoamento de Pessoal de Nível Superior (CAPES) and the Conselho Nacional de Desenvolvimento Científico e Tecnológico (CNPq).

References

[1] Vegliò F, Beolchini F. Removal of metals by biosorption: a review. Hydrometallurgy 1997;44:301–16.
[2] Volesky B. Biosorption: process modeling tools. Hydrometallurgy 2003;71:179–90.
[3] Tien CJ. Biosorption of metal ions by freshwater algae with different surface characteristics. Process Biochem 2002;38:605–13.
[4] Vegliò F, Esposito A, Reverberi AP. Copper adsorption on calcium alginate beads: equilibrium pH-related models. Hydrometallurgy 2002;69:43–57.
[5] Zouboulis AI, Loukidou MX, Matis KA. Biosorption of toxic metals from aqueous solutions by bacterial strain isolated from metal-polluted soils. Process Biochem 2004;39:909–16.
[6] Ahluwalia SS, Goyal D. Microbial and plant derived biomass for removal of heavy metals from wastewater. Bioresour Technol 2007;98:2243–57.
[7] Aksu Z. Equilibrium and kinetic modeling of cadmium (II) biosorption by *C. vulgaris* in a batch system: effect of temperature. Sep Purif Technol 2001;21:285–94.
[8] Kratochvil D, Volesky B. Advances in the biosorption of heavy metals. Tibtech 1998;16:291–300.
[9] Volesky B. Detoxification of metal-bearing effluents: biosorption for the next century. Hydrometallurgy 2001;59:203–16.
[10] Palmieri MC. Estudo da utilização de biomassas para biossorção de terras-raras. Brazil: Universidade Estadual Paulista; Ph.D. Thesis; 2001. p. 1–78.
[11] Valdman E, Erijman L, Pessoa FLP, Leite SGF. Continuous biosorption of copper and zinc by immobilized waste biomass of *Sargassum* sp. Process Biochem 2001;36:869–73.
[12] Palmieri MC, Garcia OJ, Melnikov P. Neodymium biosorption from acidic solutions in batch system. Process Biochem 2000;36:441–4.
[13] Modak JM, Natarajan KA. Biosorption of metals using nonliving biomass: a review. Miner Metall Process 1995;12:189–96.
[14] Sheng PX, Ting YP, Chen JP, Hong L. Sorption of lead, copper, cadmium, zinc, and nickel by marine algal biomass: characterization of biosorptive capacity and investigation of mechanisms. J Colloid Interface Sci 2004;275:131–41.
[15] Guibal E. Interactions of metal ions with chitosan-based sorbents: a review. Sep Purif Technol 2004;38:43–74.
[16] Yu J, Tong M, Xiaomei S, Li B. Biomass grafted with polyamic acid for enhancement of cadmium (II) and lead (II) biosorption. React Funct Polym 2007;67:564–72.
[17] Palmieri MC, Volesky B, Garcia OJ. Biosorption of lanthanum using *Sargassum fluitans* in batch system. Hydrometallurgy 2002;67:31–6.
[18] Davis TA, Volesky B, Mucci A. A review of the biochemistry of heavy metal biosorption by brown algae. Water Res 2003;37:4311–30.
[19] Draget KI, Smidsrod O, Skjak-Braek G. Alginates from algae. In: Steinbüchel A, Rhee SK, editors. Polysaccharides and polyamides in the food industry. Properties, production, and patents. Weinheim: Wiley; 2005. p. 1–29.
[20] Vijayaraghavan K, Palanivelu K, Velan M. Treatment of nickel containing electroplating effluents with *Sargassum wightii* biomass. Process Biochem 2006;41:853–9.
[21] Da Silva EA, Cossich ES, Granhen Tavares CR, Cardozo Filho L, Guirardello R. Modeling of copper(II) biosorption by marine alga *Sargassum* sp. in fixed-bed column. Process Biochem 2002;38:791–9.
[22] Valdman E, Erijman L, Pessoa FLP, Leite SGF. Continuous biosorption of Cu and Zn by immobilized waste biomass *Sargassum* sp. Process Biochem 2001;36:869–73.
[23] Martins TS, Isolani PC. Terras-raras: aplicações industriais e biológicas. Quím Nova 2005;28:111–7.
[24] Andrès Y, Thouand G, Boualam M, Mergeay M. Factors influencing the biosorption of gadolinium by microorganisms and its mobilization from sand. Appl Microbiol Biotechnol 2000;54:262–7.
[25] Rao TP, Kala R. On-line and off-line preconcentration of trace and ultratrace amounts of lanthanides. Talanta 2004;63:949–59.
[26] Diniz V, Volesky B. Biosorption of La, Eu and Yb using *Sargassum* biomass. Water Res 2005;39:239–47.
[27] Murphy W, Hughes H, McLoughlin P. Cu(II) binding by dried biomass of red, green and brown macroalgae. Water Res 2007;41:731–40.
[28] Silva JF. Análise experimental e simulação do processo de bioadsorção de metais pesados (Pb, Zn e Ni) através da alga marinha Sargassum sp. Brazil: Universidade Estadual de Campinas; PhD Thesis; 2006. p. 1–157.
[29] Fourest E, Volesky B. Contribution of sulfonate groups and alginate to heavy metal biosorption by the dry biomass of *Sargassum fluitans*. Environ Sci Technol 1995;30:277–82.
[30] Lodeiro P, Barriada JL, Herrero R, Sastre de Vicente ME. The marine macroalga *Cystoseira baccata* as biosorbent for cadmium (II) and lead (II) removal: kinetic and equilibrium studies. Environ Pollut 2006;142:264–73.

[31] Oliveira RC, Garcia Jr O. Study of biosorption of rare earth metals (La, Nd, Eu, Gd) by *Sargassum* sp. biomass in batch systems: physicochemical evaluation of kinetics and adsorption models. Adv Mater Res 2009;71–73:605–8.
[32] Gschneidner Jr KA. Physical properties of the rare earth metals. In: Lide DR, editor. CRC Handbook of Chemistry and Physics. 88th ed. Boca Raton: CRC; 2007–2008. p. 4119–24.
[33] Korenevskii AA, Sorokin VV, Karavaiko GI. Biosorption of rare earth elements. Process Metall 1999;9C:299–306.
[34] Philip L, Iyengar L, Venkobachar C. Biosorption of U, La, Pr, Nd, Eu and Dy by *Pseudomonas aeruginosa*. J Ind Microbiol Biotechnol 2000;25:1–7.
[35] Tsui MTK, Cheung KC, Tam NFY, Weng MH. A comparative study on metal sorption by brown seaweed. Chemosphere 2006;65:51–7.
[36] Oliveira RC. Estudo da concentração e recuperação de íons lantânio e neodímio por biossorção em coluna com a biomassa Sargassum sp. Brazil: Universidade Estadual Paulista; M.Sc. Thesis; 2007. p. 1–61.